Three-Dimensional Exact Analysis of Functionally Graded Laminated Composite Plates

Gennady M. Kulikov and Svetlana V. Plotnikova

Abstract A paper focuses on the implementation of the method of sampling surfaces (SaS) to three-dimensional (3D) exact solutions for functionally graded (FG) laminated composite plates. According to the SaS method, we introduce inside the nth layer I_n not equally spaced SaS parallel to the middle surface of the plate in order to choose the displacements of these surfaces as basic plate variables. This permits the presentation of the proposed FG laminated plate formulation in a very compact form. It is important that the SaS are located inside each layer at Chebyshev polynomial nodes. This fact allows one to uniformly minimize the error due to Lagrange interpolation, i.e. the use of Lagrange polynomials of high degree becomes possible. As a result, the SaS method can be applied efficiently to 3D exact solutions of elasticity for FG laminated plates with a specified accuracy utilizing the sufficient number of SaS.

1 Introduction

Nowadays, the functionally graded (FG) materials are widely used in mechanical engineering due to their advantages compared to traditional laminated materials [5, 11]. However, the study of FG plates is not a simple task because the material properties depend on the thickness coordinate and some specific assumptions regarding their variations in the thickness direction are required [9]. This fact restricts the implementation of the Pagano approach [24, 29] for the 3D exact analysis of FG simply supported rectangular plates [31]. As concerned other two popular approaches to 3D exact solutions, namely, the state space approach and the asymptotic approach they can be applied efficiently to FG plates, see Alibeigloo [1], Alibeigloo and Liew [2], Cheng and Batra [8], Reddy and Cheng [26], Zhong and Shang [33]. A new approach

G.M. Kulikov (✉) · S.V. Plotnikova
Tambov State Technical University, Sovetskaya Street, 106, Tambov 392000, Russia
e-mail: gmkulikov@mail.ru

S.V. Plotnikova
e-mail: plotnikovasvetlana62@gmail.com

H. Altenbach and G.I. Mikhasev (eds.), *Shell and Membrane Theories in Mechanics and Biology*, Advanced Structured Materials 45, DOI 10.1007/978-3-319-02535-3_13

to closed-form elasticity solutions for FG isotropic and transversely isotropic plates is presented in [10, 30]. These solutions are based on the general solution of the equilibrium equations of inhomogeneous elastic media [25]. The efficient approach to the 3D exact analysis of thermoelasticity has been proposed by Vel and Batra [27, 28]. They studied the static and transient thermoelastic problems for FG simply supported plates whose material properties and basic variables are presented by Taylor series expansions through the thickness. Ootao [22], Ootao and Ishihara [23], Ootao and Tanigawa [21] obtained the 3D exact solutions for the transient thermoelastic response of FG strips and rectangular plates with simply supported edges under nonuniform heating on outer surfaces. The original approach to analytical solutions for the FG beams and plates was developed in Altenbach and Eremeyev [4], Birsan et al. [6]. This approach is based on the so-called theory of directed curves and surfaces [3, 32], which follows the original idea of Cosserat brothers. However, the 3D exact solutions for FG laminated plates through the use of the recently developed concept of sampling surfaces (SaS) [15, 16] can not be found in the current literature. The present paper serves to fill the gap of knowledge in this research area.

The SaS approach has been already applied efficiently to 3D exact solutions of elasticity for laminated composite plates and shells [17–20]. In accordance with this method, we choose inside the nth layer I_n not equally spaced SaS $\Omega^{(n)1}$, $\Omega^{(n)2}$,..., $\Omega^{(n)I_n}$ parallel to the middle surface of the plate and introduce the displacement vectors $\mathbf{u}^{(n)1}$, $\mathbf{u}^{(n)2}$, ..., $\mathbf{u}^{(n)I_n}$ of these surfaces as basic plate variables, where $I_n \geq 3$. Such choice of unknowns in conjunction with the use of Lagrange polynomials of degree $I_n - 1$ in the thickness direction permits the presentation of governing equations of the proposed FG plate formulation in a very compact form.

An idea of using the SaS can be traced back to Kulikov [12], Kulikov and Carera [13] in which three, four and five equally spaced SaS are employed. These contributions describe the SaS approach applied to the approximate solution of 3D shell problems. It is important to note that the more general SaS approach with the arbitrary number of equally spaced SaS [14, 15] developed later by the authors does not work properly with Lagrange polynomials of high degree because of the Runge's phenomenon [7], which yields the wild oscillation at the edges of the interval when the user deals with any specific functions. If the number of equally spaced nodes is increased then the oscillations become even larger. However, the use of Chebyshev polynomial nodes inside each layer can help to improve significantly the behavior of Lagrange polynomials of high degree because such a choice allows one to minimize uniformly the error due to Lagrange interpolation.

2 Kinematic Description of Undeformed Plate

Consider a FG laminated plate of the thickness h. Let the middle surface Ω be described by Cartesian coordinates x_1 and x_2 . The coordinate x_3 is oriented in the thickness direction. The transverse coordinates of SaS inside the nth layer are defined as

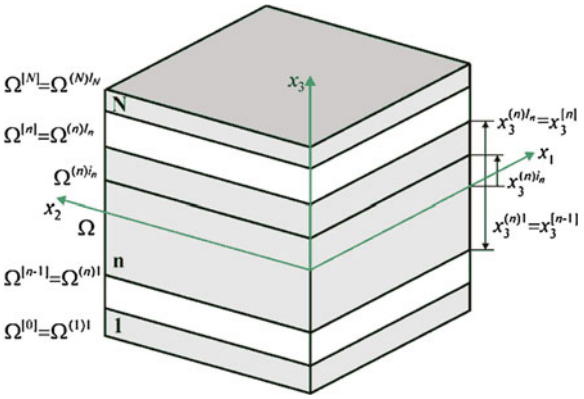

Fig. 1 Geometry of the laminated plate

$$x_3^{(n)1} = x_3^{[n-1]}, \quad x_3^{(n)I_n} = x_3^{[n]}, \tag{1}$$

$$x_3^{(n)m_n} = \frac{1}{2}\left(x_3^{[n-1]} + x_3^{[n]}\right) - \frac{1}{2}h_n \cos\left(\pi \frac{2m_n - 3}{2\,(I_n - 2)}\right), \tag{2}$$

where $x_3^{[n-1]}$ and $x_3^{[n]}$ are the transverse coordinates of layer interfaces $\Omega^{[n-1]}$ and $\Omega^{[n]}$ depicted in Fig. 1; $h_n = x_3^{[n]} - x_3^{[n-1]}$ is the thickness of the nth layer; I_n is the number of SaS corresponding to the nth layer; the index n identifies the belonging of any quantity to the nth layer and runs from 1 to N; N is the total number of layers; the index m_n identifies the belonging of any quantity to the inner SaS of the nth layer and runs from 2 to $I_n - 1$, whereas the indices i_n, j_n, k_n to be introduced later for describing all SaS of the nth layer run from 1 to I_n. Besides, the tensorial indices i, j, k, l range from 1 to 3 and Greek indices α, β range from 1 to 2. It is worth noting that the transverse coordinates of inner SaS Eq. (2) coincide with the coordinates of Chebyshev polynomial nodes [7]. This fact has a great meaning for the convergence of the SaS method [16–18].

3 Kinematic Description of Deformed Plate

The components of the strain tensor ε_{ij} are written as

$$2\varepsilon_{ij} = u_{i,j} + u_{j,i}, \tag{3}$$

where u_i are the displacements of the plate.

We start now with the first assumption of the proposed FG laminated plate formulation. Let us assume that the displacement and strain fields are distributed through the thickness of the nth layer as follows:

$$u_i^{(n)} = \sum_{i_n} L^{(n)i_n} u_i^{(n)i_n}, \quad x_3^{[n-1]} \le x_3 \le x_3^{[n]}, \tag{4}$$

$$\varepsilon_{ij}^{(n)} = \sum_{i_n} L^{(n)i_n} \varepsilon_{ij}^{(n)i_n}, \quad x_3^{[n-1]} \le x_3 \le x_3^{[n]}, \tag{5}$$

where $u_i^{(n)i_n}(x_1, x_2)$ are the displacements of SaS of the nth layer $\Omega^{(n)i_n}$, $\varepsilon_{ij}^{(n)i_n}(x_1, x_2)$ are the strains of the same SaS; $L^{(n)i_n}(x_3)$ are the Lagrange polynomials of degree $I_n - 1$ defined as

$$u_i^{(n)i_n} = u_i\left(x_3^{(n)i_n}\right), \tag{6}$$

$$\varepsilon_{ij}^{(n)i_n} = \varepsilon_{ij}\left(x_3^{(n)i_n}\right), \tag{7}$$

$$L^{(n)i_n} = \prod_{j_n \ne i_n} \frac{x_3 - x_3^{(n)j_n}}{x_3^{(n)i_n} - x_3^{(n)j_n}}. \tag{8}$$

The use of relations (3), (6) and (7) yields

$$2\varepsilon_{\alpha\beta}^{(n)i_n} = u_{\alpha,\beta}^{(n)i_n} + u_{\beta,\alpha}^{(n)i_n}, \tag{9}$$

$$2\varepsilon_{\alpha 3}^{(n)i_n} = \beta_\alpha^{(n)i_n} + u_{3,\alpha}^{(n)i_n}, \tag{10}$$

$$\varepsilon_{33}^{(n)i_n} = \beta_3^{(n)i_n}, \tag{11}$$

$$\beta_i^{(n)i_n} = u_{i,3}\left(x_3^{(n)i_n}\right), \tag{12}$$

where $\beta_i^{(n)i_n}(x_1, x_2)$ are the values of derivatives of displacements with respect to transverse coordinate x_3 at SaS defined according to Eq. (4) as

$$\beta_i^{(n)i_n} = \sum_{j_n} M^{(n)j_n}\left(x_3^{(n)i_n}\right) u_i^{(n)j_n}, \tag{13}$$

where $M^{(n)j_n} = L_{,3}^{(n)j_n}$ are the derivatives of Lagrange polynomials, which are calculated at SaS as follows:

$$M^{(n)j_n}\left(x_3^{(n)i_n}\right) = \frac{1}{x_3^{(n)j_n} - x_3^{(n)i_n}} \prod_{k_n \neq i_n, j_n} \frac{x_3^{(n)i_n} - x_3^{(n)k_n}}{x_3^{(n)j_n} - x_3^{(n)k_n}} \quad \text{for} \quad j_n \neq i_n,$$

$$M^{(n)i_n}\left(x_3^{(n)i_n}\right) = -\sum_{j_n \neq i_n} M^{(n)j_n}\left(x_3^{(n)i_n}\right). \tag{14}$$

This means that the key functions $\beta_i^{(n)i_n}$ of the proposed FG laminated plate formulation are represented as a linear combination of displacements of SaS of the nth layer $u_i^{(n)j_n}$.

4 Variational Formulation

The variational equation for the FG laminated plate in the case of conservative loading can be written as

$$\delta \Pi = 0, \tag{15}$$

where Π is the total potential energy given by

$$\Pi = \frac{1}{2} \iint_{\Omega} \sum_{n} \int_{x_3^{[n-1]}}^{x_3^{[n]}} \sigma_{ij}^{(n)} \varepsilon_{ij}^{(n)} dx_1 dx_2 dx_3 - W, \tag{16}$$

$$W = \iint_{\Omega} \left(p_i^{+} u_i^{[N]} - p_i^{-} u_i^{[0]} \right) dx_1 dx_2 + W_{\Sigma}, \tag{17}$$

where $\sigma_{ij}^{(n)}$ are the components of the stress tensor of the nth layer; $u_i^{[0]} = u_i^{(1)1}$ and $u_i^{[N]} = u_i^{(N)I_N}$ are the displacements of bottom and top surfaces $\Omega^{[0]}$ and $\Omega^{[N]}$; p_i^{-} and p_i^{+} are the loads acting on bottom and top surfaces; W_{Σ} is the work done by external loads applied to the edge surface Σ .

Substituting the strain distribution (5) in (16) and introducing stress resultants

$$H_{ij}^{(n)i_n} = \int_{x_3^{[n-1]}}^{x_3^{[n]}} \sigma_{ij}^{(n)} L^{(n)i_n} dx_3, \tag{18}$$

one obtains

$$\Pi = \frac{1}{2}\iint\limits_{\Omega}\sum_{n}\sum_{i_n} H_{ij}^{(n)i_n}\varepsilon_{ij}^{(n)i_n}dx_1dx_2 - W. \tag{19}$$

The second assumption of the FG laminated plate formulation is quite standard and consists in the following:

$$\boldsymbol{\sigma}_{ij}^{(n)} = C_{ijkl}^{(n)}\varepsilon_{kl}^{(n)}, \quad x_3^{[n-1]} \le x_3 \le x_3^{[n]}, \tag{20}$$

where $C_{ijkl}^{(n)}$ are the elastic constants of the nth layer.

Next, we introduce the third and last assumption. Let us assume that elastic constants are distributed through the thickness of a plate as follows:

$$C_{ijkl}^{(n)} = \sum_{i_n} L^{(n)i_n} C_{ijkl}^{(n)i_n}, \tag{21}$$

where $C_{ijkl}^{(n)i_n}$ are the values of elastic constants on SaS of the nth layer.

Substituting constitutive Eq. (20) in (18) and taking into account the through-thickness distributions (5) and (21), we have

$$H_{ij}^{(n)i_n} = \sum_{j_n,k_n} \Lambda^{(n)i_n j_n k_n} C_{ijkl}^{(n)j_n}\varepsilon_{kl}^{(n)k_n}, \tag{22}$$

where

$$\Lambda^{(n)i_n j_n k_n} = \int\limits_{x_3^{[n-1]}}^{x_3^{[n]}} L^{(n)i_n} L^{(n)j_n} L^{(n)k_n} dx_3. \tag{23}$$

5 3D Exact Solution for Functionally Graded Laminated Plates

In this section, we study a simply supported FG laminated orthotropic rectangular plate. The edge boundary conditions of the plate are written as

$$\begin{aligned} &\boldsymbol{\sigma}_{11}^{(n)} = u_2^{(n)} = u_3^{(n)} = 0 \quad \text{at} \quad x_1 = 0 \quad \text{and} \quad x_1 = a, \\ &\boldsymbol{\sigma}_{22}^{(n)} = u_1^{(n)} = u_3^{(n)} = 0 \quad \text{at} \quad x_2 = 0 \quad \text{and} \quad x_2 = b, \end{aligned} \tag{24}$$

where a and b are the plate dimensions. To satisfy boundary conditions, we search the analytical solution of the problem by a method of the double Fourier series expansion

$$u_1^{(n)i_n} = \sum_{r,s} u_{1rs}^{(n)i_n} \cos\frac{r\pi x_1}{a} \sin\frac{s\pi x_2}{b},$$
$$u_2^{(n)i_n} = \sum_{r,s} u_{2rs}^{(n)i_n} \sin\frac{r\pi x_1}{a} \cos\frac{s\pi x_2}{b}, \tag{25}$$
$$u_3^{(n)i_n} = \sum_{r,s} u_{3rs}^{(n)i_n} \sin\frac{r\pi x_1}{a} \sin\frac{s\pi x_2}{b},$$

where r, s are the wave numbers in plane directions. The external loads are also expanded in double Fourier series.

Substituting (25) and Fourier series corresponding to mechanical loading into the total potential energy (17) and (19) with $W_\Sigma = 0$ and allowing for relations (9), (10), (11), (13) and (22), one obtains

$$\Pi = \sum_{r,s} \Pi_{rs}\left(u_{irs}^{(n)i_n}\right). \tag{26}$$

Invoking the variational Eqs. (15), (26), we arrive at the system of linear algebraic equations

$$\frac{\partial \Pi_{rs}}{\partial u_{irs}^{(n)i_n}} = 0 \tag{27}$$

of order

$$3\left(\sum_n I_n - N + 1\right).$$

The linear system (27) can be easily solved by using a method of Gaussian elimination.

The described algorithm was performed with the Symbolic Math Toolbox, which incorporates symbolic computations into the numeric environment of MATLAB. Such a technique gives the possibility to derive the exact solutions of 3D elasticity for FG laminated orthotropic plates with a specified accuracy.

5.1 Single-Layer Square Plate

Consider a FG single-layer square plate subjected to transverse sinusoidal loading acting on its top surface

$$p_3^+ = p_0 \sin\frac{\pi x_1}{a} \sin\frac{\pi x_2}{b}, \tag{28}$$

where $p_0 = 1$ Pa and $a = b = 1$ m.

It is assumed that the elastic modulus is distributed in the thickness direction according to the exponential law:

$$E = E^+ e^{\alpha(z-0.5)}, \quad z = x_3/h, \tag{29}$$

where E^+ is the Young modulus on the top surface; α is the material gradient index defined by

$$\alpha = \ln\left(\frac{E^+}{E^-}\right), \tag{30}$$

where E^- is the Young modulus on the bottom surface, whereas the Poisson ratio ν is constant through the thickness [10]. The material parameters are taken to be $E^+ = 10^7$ Pa and $\nu = 0.3$. To compare the results derived with closed-form solutions [10, 29], the following dimensionless variables are introduced:

$$\bar{u}_1 = G^+ u_1(0, a/2, z)/hp_0, \quad \bar{u}_3 = G^+ u_3(a/2, a/2, z)/hp_0,$$
$$\bar{\sigma}_{11} = \sigma_{11}(a/2, a/2, z)/p_0, \quad \bar{\sigma}_{12} = \sigma_{12}(0, 0, z)/p_0,$$
$$\bar{\sigma}_{13} = \sigma_{13}(0, a/2, z)/p_0, \quad \bar{\sigma}_{33} = \sigma_{33}(a/2, a/2, z)/p_0,$$

where $G^+ = E^+/(2(1+\nu))$ is the shear modulus on the top surface.

Tables 1, 2, 3, 4 show the results of a convergence study due to increasing the number of SaS. As it turned out, the SaS method provides 15 right digits for all basic variables (in fact, the better accuracy is possible) utilizing 13 inner SaS inside the plate body. It should be noted that herein the bottom and top surfaces are not included into a set of SaS because the use of Chebyshev polynomial nodes allows one to minimize uniformly the error due to Lagrange interpolation. Figure 2 displays the distributions of transverse stresses in the thickness direction for the slenderness ratio $a/h = 1$ employing 11 SaS. These results demonstrate convincingly the high potential of the proposed FG plate formulation because boundary conditions on the bottom and top surfaces of the plate for transverse stresses are satisfied exactly.

5.2 Three-Layer Square Plate

Here, we study a three-layer square plate subjected to sinusoidally distributed transverse loading (28). The outer layers with equal thicknesses $h_1 = h_3 = h/4$ are composed of the graphite-epoxy composite with Young moduli $E_1 = 172.72$ GPa, $E_2 = E_3 = 6.909$ GPa, shear moduli $G_{12} = G_{13} = 3.45$ GPa, $G_{23} = 1.38$ GPa and Poisson ratios $\nu_{12} = \nu_{13} = \nu_{23} = 0.25$. It is assumed that fibers of the bottom and top layers are oriented respectively in x_1- and x_2-directions. The central layer is made of the FG transversely isotropic material whose elastic constants are distributed in the thickness direction according to a power law:

Table 1 Results for a single-layer square plate with $a/h = 3$ and $\alpha = 0$

I_1	$-\bar{u}_1(0.5)$	$\bar{u}_3(0.5)$	$\bar{\sigma}_{11}(0.5)$	$-\bar{\sigma}_{12}(0.5)$	$\bar{\sigma}_{13}(0)$	$\bar{\sigma}_{33}(0)$
3	0.3986372494504680	1.278878243389591	1.999302146854837	0.8349039028805547	0.4977436151168003	0.4752837277628003
7	0.4358933937131948	1.342554953466513	2.124032428288413	0.9129329889584641	0.7022762666060094	0.4943950643281928
11	0.4358933942603120	1.342554689543095	2.124018410314048	0.9129329901043438	0.7023022083223538	0.4944039935419638
15	0.4358933942603121	1.342554689542491	2.124018410193782	0.9129329901043439	0.7023022084767580	0.4944039936052152
19	0.4358933942603120	1.342554689542491	2.124018410193780	0.9129329901043437	0.7023022084767578	0.4944039936052150
Exact[a]	0.4358933942603120	1.342554689542491	2.124018410193781	0.9129329901043437	0.7023022084767578	0.4944039936052149

[a] The exact results have been obtained by the authors using the Vlasov's closed-form solution

Table 2 Results for a single-layer square plate with $a/h = 3$ and $\alpha = 0.1$

I_1	$-\bar{u}_1(0.5)$	$\bar{u}_3(0.5)$	$\bar{\boldsymbol{\sigma}}_{11}(0.5)$	$-\bar{\boldsymbol{\sigma}}_{12}(0.5)$	$\bar{\boldsymbol{\sigma}}_{13}(0)$	$\bar{\boldsymbol{\sigma}}_{33}(0)$
3	0.4158336502652652	1.347977241257294	2.073239906807475	0.8700097684529745	0.4983226799021384	0.4596565434470269
7	0.4536977979133792	1.414636043682728	2.193265858989844	0.9502222750248108	0.7020700339720654	0.4877173446168515
11	0.4536977984142576	1.414635771310962	2.193270258459039	0.9502224469642998	0.7020957676355946	0.4877129579452970
15	0.4536977984142576	1.414635771310368	2.193270258650021	0.9502224469653965	0.7020957677904856	0.4877129578319663
19	0.4536977984142575	1.414635771310368	2.193270258650021	0.9502224469653963	0.7020957677904854	0.4877129578319657
Exact		1.41464				

Table 3 Results for a single-layer square plate with $a/h = 10$ and $\alpha = 0$

I_1	$-\bar{u}_1(0.5)$	$\bar{u}_3(0.5)$	$\bar{\sigma}_{11}(0.5)$	$-\bar{\sigma}_{12}(0.5)$	$\bar{\sigma}_{13}(0)$	$\bar{\sigma}_{33}(0)$
3	16.69442044348862	112.4420178073405	19.91690124596434	10.48941372424062	1.706202131658078	0.4978329738513218
7	16.81014395019634	113.1720941024937	20.04394635519068	10.56212494794475	2.383373139214406	0.4999497585886086
11	16.81014395019644	113.1720941004914	20.04394633189751	10.56212494794481	2.383373791176881	0.4999497657893389
15	16.81014395019644	113.1720941004913	20.04394633189750	10.56212494794481	2.383373791176909	0.4999497657893389
19	16.81014395019645	113.1720941004914	20.04394633189751	10.56212494794481	2.383373791176910	0.4999497657893400
Exact[a]	16.81014395019644	113.1720941004914	20.04394633189751	10.56212494794481	2.383373791176911	0.4999497657893391

[a] The exact results have been obtained by the authors using the Vlasov's closed-form solution

Table 4 Results for a single-layer square plate with $a/h = 10$ and $\alpha = 0.1$

I_1	$-\bar{u}_1(0.5)$	$\bar{u}_3(0.5)$	$\bar{\boldsymbol{\sigma}}_{11}(0.5)$	$-\bar{\boldsymbol{\sigma}}_{12}(0.5)$	$\bar{\boldsymbol{\sigma}}_{13}(0)$	$\bar{\boldsymbol{\sigma}}_{33}(0)$
3	17.27349261247991	118.2552720004223	20.59552826078969	10.84973560354474	1.706517604171541	0.4818430337132246
7	17.39081000813009	119.0218924804116	20.72151070605207	10.92696818763486	2.383067071421124	0.4936497163566589
11	17.39081000813025	119.0218924788537	20.72151235713497	10.92696819230357	2.383067798660550	0.4936485236803348
15	17.39081000813025	119.0218924788537	20.72151235713520	10.92696819230357	2.383067798660592	0.4936485236802035
19	17.39081000813026	119.0218924788537	20.72151235713521	10.92696819230358	2.383067798660592	0.4936485236802040

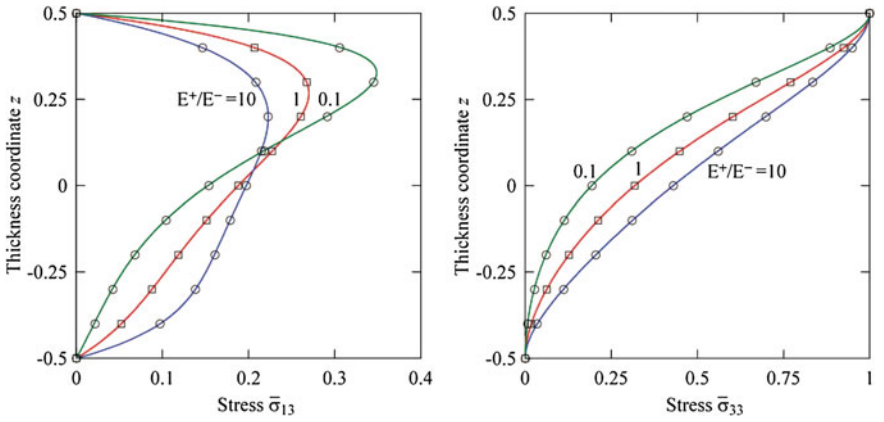

Fig. 2 Distributions of transverse stresses through the thickness of the plate with $a/h = 1$: present analysis (-) for $I_1 = 11$ and analytical solutions [10] (◯) and [29] (□)

$$C_{ijkl} = C^{-}_{ijkl} V^{-} + C^{+}_{ijkl} V^{+},$$
$$V^{+} = 1 - V^{-}, \quad V^{-} = (0.5 - 2z)^{\gamma}, \quad -0.25 \le z \le 0.25, \tag{31}$$

where C^{-}_{ijkl} and C^{+}_{ijkl} are the values of elastic constants on the bottom and top surfaces; γ is the material gradient index; $z = x_3/h$ is the dimensionless thickness coordinate. The elastic constants on the bottom surface are considered to be the same as those in Woodward and Kashtalyan [30]:

$$C^{-}_{1111} = C^{-}_{2222} = 41.3\,\text{GPa}, \quad C^{-}_{1122} = 14.7\,\text{GPa}, \quad C^{-}_{1133} = C^{-}_{2233} = 10.1\,\text{GPa},$$

$$C^{-}_{3333} = 36.2\,\text{GPa}, \quad C^{-}_{1313} = C^{-}_{2323} = 10.0\,\text{GPa}, \quad C^{-}_{1212} = 13.3\,\text{GPa},$$

whereas the elastic constants on the top surface are taken as $C^{+}_{ijkl} = 2C^{-}_{ijkl}$. The distribution of elastic constants through the thickness of the FG layer for three values of the material gradient index $\gamma = 1, 2$ and 5 is shown in Fig. 3.

The geometric parameters of the plate are chosen to be $a = b = 1\text{m}$, $h_1 = h_3 = h/4$ and $h_2 = h/2$. To analyze the derived results efficiently, we introduce the following dimensionless variables:

$$\bar{u}_1 = E_1 u_1(0, a/2, z)/hp_0, \quad \bar{u}_2 = E_1 u_2(a/2, 0, z)/hp_0,$$
$$\bar{u}_3 = E_1 u_3(a/2, a/2, z)/hp_0,$$
$$\bar{\boldsymbol{\sigma}}_{11} = \boldsymbol{\sigma}_{11}(a/2, a/2, z)/p_0, \quad \bar{\boldsymbol{\sigma}}_{22} = \boldsymbol{\sigma}_{22}(a/2, a/2, z)/p_0,$$

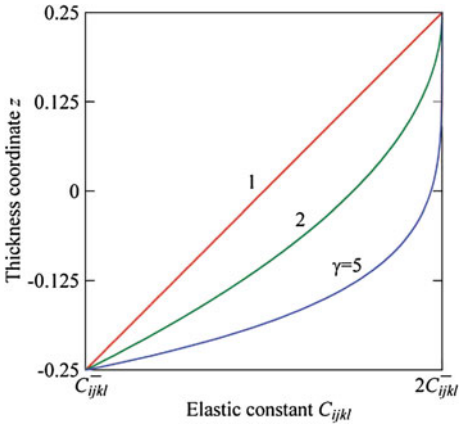

Fig. 3 Distribution of elastic constants through the thickness of the central FG layer

Table 5 Results for a FG three-layer square plate for $a/h = 2$ and $\gamma = 2$

I_n	$-\bar{u}_1(0.5)$	$\bar{u}_3(0.5)$	$\bar{\sigma}_{11}(0.5)$	$\bar{\sigma}_{22}(0.5)$	$-\bar{\sigma}_{12}(0.5)$	$\bar{\sigma}_{13}(0)$	$\bar{\sigma}_{23}(0)$	$\bar{\sigma}_{33}(0)$
3	3.1521	12.771	0.48242	2.4846	0.14094	0.55566	0.49464	0.43914
5	3.2011	12.835	0.47688	2.5322	0.14363	0.61857	0.57944	0.45240
7	3.2012	12.835	0.47647	2.5318	0.14364	0.61804	0.57621	0.45157
9	3.2012	12.835	0.47646	2.5318	0.14364	0.61796	0.57638	0.45156
11	3.2012	12.835	0.47646	2.5318	0.14364	0.61797	0.57637	0.45156
13	3.2012	12.835	0.47646	2.5318	0.14364	0.61797	0.57637	0.45156

Table 6 Results for a FG three-layer square plate for $a/h = 10$ and $\gamma = 2$

I_n	$-\bar{u}_1(0.5)$	$\bar{u}_3(0.5)$	$\bar{\sigma}_{11}(0.5)$	$\bar{\sigma}_{22}(0.5)$	$-\bar{\sigma}_{12}(0.5)$	$\bar{\sigma}_{13}(0)$	$\bar{\sigma}_{23}(0)$	$\bar{\sigma}_{33}(0)$
3	418.69	1969.8	5.9874	46.783	3.5268	2.8096	2.2369	0.48787
5	418.93	1970.7	5.9825	46.799	3.5288	2.9551	2.5383	0.50494
7	418.93	1970.7	5.9825	46.799	3.5288	2.9655	2.5325	0.50435
9	418.93	1970.7	5.9825	46.799	3.5288	2.9655	2.5329	0.50436
11	418.93	1970.7	5.9825	46.799	3.5288	2.9655	2.5329	0.50436

$$\bar{\sigma}_{33} = \sigma_{33}(a/2, a/2, z)/p_0, \quad \bar{\sigma}_{12} = \sigma_{12}(0, 0, z)/p_0,$$
$$\bar{\sigma}_{13} = \sigma_{13}(0, a/2, z)/p_0, \quad \bar{\sigma}_{23} = \sigma_{23}(a/2, 0, z)/p_0.$$

Tables 5 and 6 show that the SaS method allows the derivation of the 3D exact solution of elasticity for thick FG laminated composite plates with a prescribed

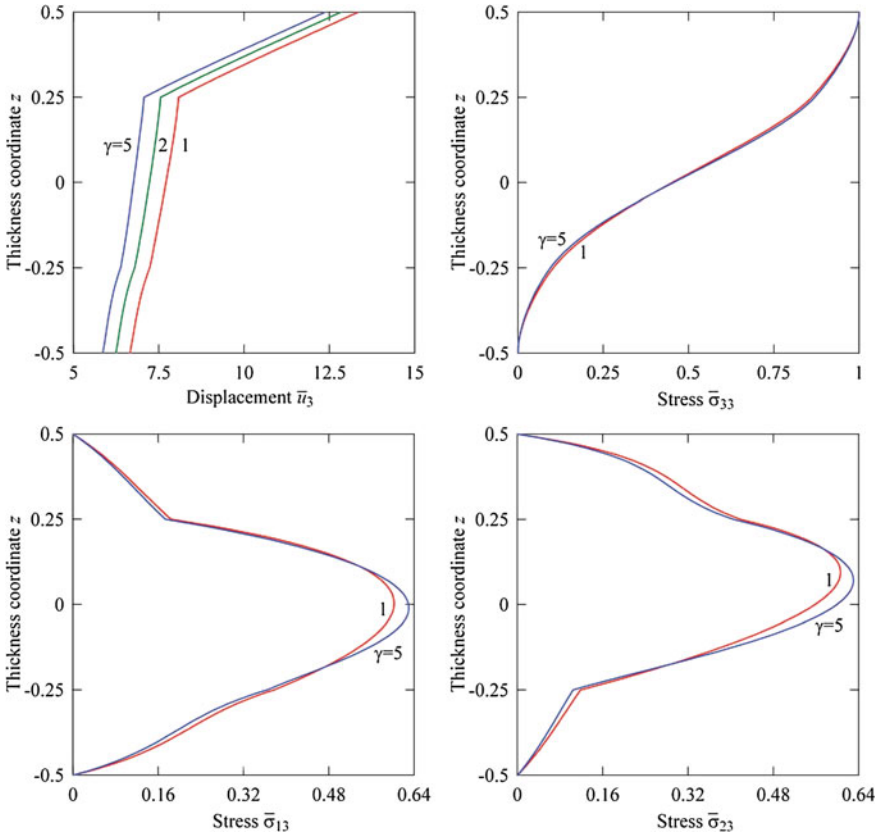

Fig. 4 Distributions of the transverse displacement and transverse stresses through the thickness of the FG three-layer plate with $a/h = 2$ and $\gamma = 1, 2, 5$

accuracy by using the large number of SaS inside each layer. Figures 4, 5 and 6 present the distributions of the transverse displacement and transverse stresses through the thickness of the plate for different values of the material gradient index γ employing 13 SaS for each layer. As can be seen, the boundary conditions on outer surfaces are satisfied again properly. The similar conclusion can be made concerning the continuity conditions at layer interfaces.

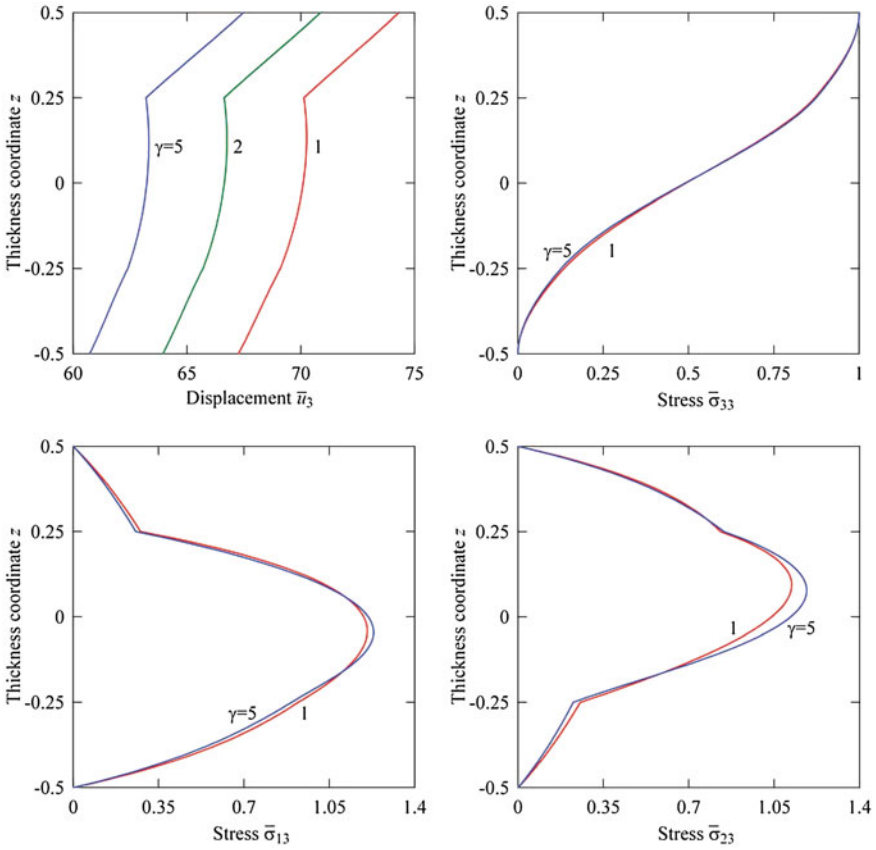

Fig. 5 Distributions of the transverse displacement and transverse stresses through the thickness of the FG three-layer plate with $a/h = 4$ and $\gamma = 1, 2, 5$

6 Conclusions

An efficient approach to 3D elasticity solutions for FG laminated plates has been proposed. It is based on the recently developed method of SaS located at Chebyshev polynomial nodes inside each layer of the plate and layer interfaces as well. The stress analysis is based on the 3D constitutive equations of elasticity and gives an opportunity to obtain the 3D exact solutions for thick and thin FG laminated composite plates with a specified accuracy.

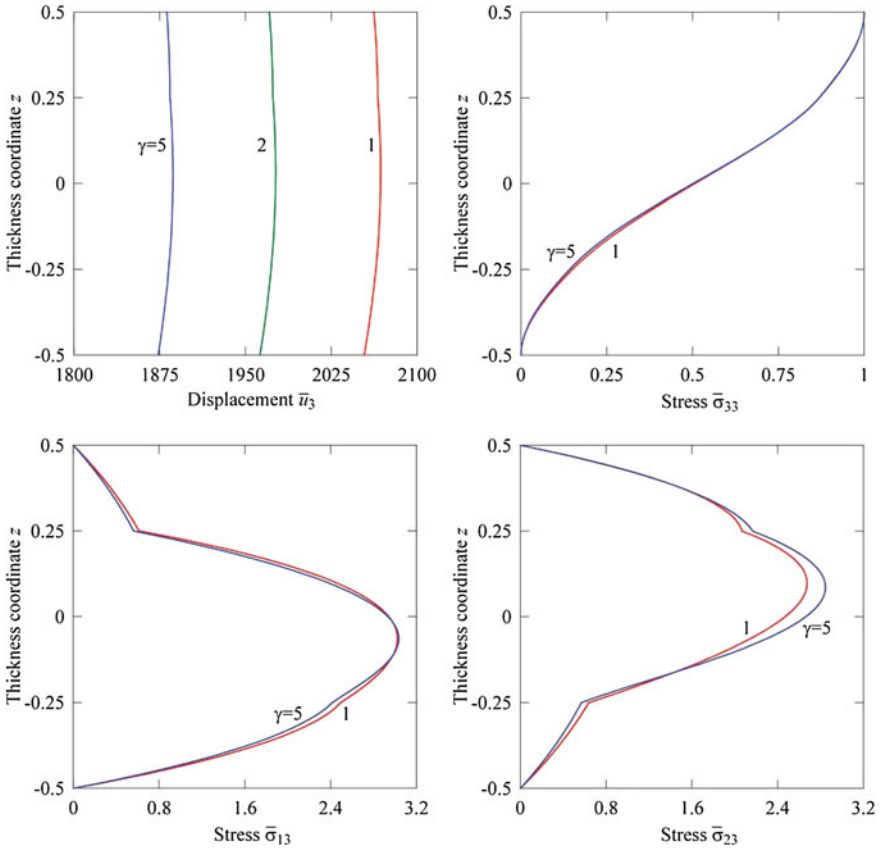

Fig. 6 Distributions of the transverse displacement and transverse stresses through the thickness of the FG three-layer plate with $a/h = 10$ and $\gamma = 1, 2, 5$

Acknowledgments This work was supported by Russian Ministry of Education and Science under Grant No. 9.137.2014K and by Russian Foundation for Basic Research under Grant No 13-01-00155.

References

1. Alibeigloo, A.: Exact solution for thermo-elastic response of functionally graded rectangular plates. Compos. Struct. **92**, 113–121 (2010)
2. Alibeigloo, A., Liew, K.M.: Thermoelastic analysis of functionally graded carbon nanotube-reinforced composite plate using theory of elasticity. Compos. Struct. **106**(3), 873–881 (2013)
3. Altenbach, H., Naumenko, K., Zhilin, P.A.: A direct approach to the formulation of constitutive equations for rods and shells. In: Pietraszkiewicz, W., Szymczak, C. (eds.) Shell Structures:

Theory and Applications, pp. 87–90. Taylor and Francis, London (2006)
4. Altenbach, H., Eremeyev, V.A.: Direct approach-based analysis of plates composed of functionally graded materials. Arch. Appl. Mech. **78**, 775–794 (2008)
5. Birman, V., Byrd, L.W.: Modeling and analysis of functionally graded materials and structures. Appl. Mech. Rev. **60**, 195–216 (2007)
6. Birsan, M., Altenbach, H., Sadowski, T., Eremeyev, V.A., Pietras, D.: Deformation analysis of functionally graded beams by the direct approach. Compos. B **43**, 1315–1328 (2012)
7. Burden, R.L., Faires, J.D.: Numerical Analysis, 9th edn. Brooks/Cole, Boston (2010)
8. Cheng, Z.Q., Batra, R.C.: Three-dimensional thermoelastic deformations of a functionally graded elliptic plate. Compos. B **31**, 97–106 (2000)
9. Jha, D.K., Kant, T., Singh, R.K.: A critical review of recent research on functionally graded plates. Compos. Struct. **96**, 833–849 (2013)
10. Kashtalyan, M.: Three-dimensional elasticity solution for bending of functionally graded rectangular plates. Eur. J. Mech. A. Solids **23**, 853–864 (2004)
11. Koizumi, M.: FGM activities in Japan. Compos. B **28**, 1–4 (1997)
12. Kulikov, G.M.: Refined global approximation theory of multilayered plates and shells. J. Eng. Mech. **127**, 119–125 (2001)
13. Kulikov, G.M., Carrera, E.: Finite deformation higher-order shell models and rigid-body motions. Int. J. Solids Struct. **45**, 3153–3172 (2008)
14. Kulikov, G.M., Plotnikova, S.V.: On the use of a new concept of sampling surfaces in a shell theory. Adv. Struct. Mater. **15**, 715–726 (2011a)
15. Kulikov, G.M., Plotnikova, S.V.: Solution of static problems for a three-dimensional elastic shell. Dokl. Phys. **56**, 448–451 (2011b)
16. Kulikov, G.M., Plotnikova, S.V.: On the use of sampling surfaces method for solution of 3D elasticity problems for thick shells. ZAMM **92**, 910–920 (2012b)
17. Kulikov, G.M., Plotnikova, S.V.: Exact 3D stress analysis of laminated composite plates by sampling surfaces method. Compos. Struct. **94**, 3654–3663 (2012a)
18. Kulikov, G.M., Plotnikova, S.V.: Advanced formulation for laminated composite shells: 3D stress analysis and rigid-body motions. Compos. Struct. **95**, 236–246 (2013a)
19. Kulikov, G.M., Plotnikova, S.V.: Three-dimensional exact analysis of piezoelectric laminated plates via a sampling surfaces method. Int. J. Solids Struct. **50**, 1916–1929 (2013c)
20. Kulikov, G.M., Plotnikova, S.V.: A sampling surfaces method and its application to three-dimensional exact solutions for piezoelectric laminated shells. Int. J. Solids Struct. **50**, 1930–1943 (2013b)
21. Ootao, Y., Tanigawa, Y.: Three-dimensional solution for transient thermal stresses of an orthotropic functionally graded rectangular plate. Compos. Struct. **80**, 10–20 (2007)
22. Ootao, Y.: Transient thermoelastic analysis for a multilayered thick strip with piecewise exponential nonhomogeneity. Compos. B **42**, 973–981 (2011)
23. Ootao, Y., Ishihara, M.: Three-dimensional solution for transient thermoelastic problem of a functionally graded rectangular plate with piecewise exponential law. Compos. Struct. **106**, 672–680 (2013)
24. Pagano, N.J.: Exact solutions for rectangular bidirectional composites and sandwich plates. J. Compos. Mater. **4**, 20–34 (1970)
25. Plevako, V.P.: On the theory of elasticity of inhomogeneous media. J. Appl. Math. Mech. **35**, 806–813 (1971)
26. Reddy, J.N., Cheng, Z.Q.: Three-dimensional thermomechanical deformations of functionally graded rectangular plates. Eur. J. Mech. A. Solids **20**, 841–855 (2001)
27. Vel, S.S., Batra, R.C.: Exact solution for thermoelastic deformations of functionally graded thick rectangular plates. AIAA J. **40**, 1421–1433 (2002)
28. Vel, S.S., Batra, R.C.: Three-dimensional analysis of transient thermal stresses in functionally graded plates. Int. J. Solids Struct. **40**, 7181–7196 (2003)
29. Vlasov, B.F.: On the bending of a rectangular thick plate (in Russ.). Vestnik. Moskov. Univ. Ser. Mat. Mekh. **2**, 25–31 (1957)

30. Woodward, B., Kashtalyan, M.: Three-dimensional elasticity solution for bending of transversely isotropic functionally graded plates. Eur. J. Mech. A. Solids **30**, 705–718 (2011)
31. Wu, C., Chiu, K., Wang, Y.: A review on the three-dimensional analytical approaches of multilayered and functionally graded piezoelectric plates and shells. Comput. Mater. Continua. **8**, 93–132 (2008)
32. Zhilin, P.: Mechanics of deformable directed surfaces. Int. J. Solids Struct. **12**, 635–648 (1976)
33. Zhong, Z., Shang, E.: Three-dimensional exact analysis of a simply supported functionally gradient piezoelectric plate. Int. J. Solids Struct. **40**, 5335–5352 (2003)